

## A STATISTICAL MODEL FOR CONTACT ORIENTATION AND ANISOTROPY IN GRANULAR ASSEMBLIES

Chun-Qing Hu<sup>1</sup>, Hong-Wu Song<sup>1</sup>, Hai Liu<sup>1,2</sup>, D. Banabic<sup>3</sup>, Shi-Hong Zhang<sup>1</sup>, Ming Cheng<sup>1</sup>, Shuai-Feng Chen<sup>1</sup>

<sup>1</sup> Institute of Metal Research, Chinese Academy of Sciences, 72 Wenhua Road, Shenyang 110016, China

<sup>2</sup> Shenyang Polytechnic College, 32 Laodong Road, Shenyang 110016, China

<sup>3</sup> Technical University of Cluj-Napoca, Str. Memorandumului, 28, 400114, Cluj-Napoca, Romania

Corresponding author: Dr. Hong-Wu Song, E-mail: hwsong@imr.ac.cn

**Abstract:** The spatial distribution of contact orientations and anisotropy in granular assemblies stand for the directional features of contacts and contact forces. Contact anisotropy and contact force anisotropy are two fundamental concepts for microscopic and macroscopic mechanics of granular materials. In this paper, a kind of diagrammatic description for illustrating anisotropy in granular assemblies, named contact orientation distribution diagram (CODD), is proposed. A group of statistical indicators are developed to determine anisotropies. As a result, contact anisotropies and contact force anisotropies in different granular assemblies which are simulated with different existing methods, under different boundaries and using different densification procedures are compared and discussed.

**Key words:** granular materials, contact orientation, contact anisotropy, contact force anisotropy.

### 1. INTRODUCTION

Since the inception of research on granular materials, contact between particles inside has been intensively focused on with great interest and expectation all the time, such as coordination number (Bernal and Mason, 1960; Agnolin and Roux, 2007), contact forces (Liu *et al.*, 1995; Kruyt and Rothenburg, 2002; Bagi, 2003; Trentadue, 2011), contact network (Liu *et al.*, 2015; Radjai *et al.*, 1996; Silbert *et al.*, 2002), etc. Contact is the most fundamental property and produces some unusual features of granular materials.

Intergranular contact is microscopic characteristics of granular materials and is always used as basic element to construct theories and models (Nemat-Nasser, 2000; He, 2014). As an essential parameter of contact, contact orientation can interact with contact anisotropy and contact force anisotropy to impact on mechanical behaviors of granular materials (Horne, 1965; Ouadfel and Rothenburg, 2001; Majmudar and Behringer, 2005). In some configurations contact orientation can also produce indirect interactions with other parameters. For example, in configuration of inertial granular flows, coordination number and inertial number indirectly interact with contact orientation (Azema and Radjai, 2014). Obviously, isotropy and anisotropy of granular materials significantly depend on the contact orientation. It has been revealed in several publications that induced anisotropy in contact orientations plays a key role in microscopic behavior of cohesionless granular materials (Cundall *et al.*, 1982; Thornton and Barnes, 1986; Rothenburg and Bathurst, 1989). In this paper, contact orientation and anisotropy in granular assemblies are focused on and discussed.

In accordance with Cundall and Strack analysis (Cundall and Strack, 1983), two types of anisotropies are defined: fabric anisotropy (*i.e.* contact anisotropy above) and anisotropy in contact forces (*i.e.* contact force anisotropy above). Contact anisotropy denotes directions of contact normals and is necessary for the link between macroscopic stress tensor and microscopic contact forces. Contact force anisotropy denotes direction-dependent deviations of contact forces from the mean and is associated with the deviatoric part of the stress tensor. It can be seen from the definition that contact anisotropy is a kind of ‘geometrical’ anisotropy of contacts and contact force anisotropy is ‘mechanical’ anisotropy. Because of large quantities of contacts in granular assemblies, a statistics of contact orientations is necessary and practicable. Following the works of Horne, Ouadfel, Rothenburg, etc., in the case that the entire orientation domain is divided into a number of equal intervals, contact anisotropy can be represented as probability distribution of contact normals over all the

orientation intervals, and contact force anisotropy can be expressed as distribution of ratio of average contact forces in each orientation interval and overall orientation intervals (Horne, 1965; Ouadfel and Rothenburg, 2001).

To characterize contact orientation distribution, in section 2, a diagrammatic description referred to as contact orientation distribution diagram (CODD) is introduced and a statistical anisotropy model for cohesionless granular materials is proposed. Based on the statistical anisotropy model, in section 3, anisotropies in different particle arrangements (different generating approaches, boundaries and densification procedures) are compared and discussed. Some important conclusions are presented in section 5.

## 2. STATISTICAL ANISOTROPY MODEL

### 2.1. Contact orientation distribution diagram (CODD)

In spherical coordinates, orientation can be parametrized by its zenith angle  $\varphi$  and azimuth angle  $\theta$ . Here stereographic projection is introduced to characterize orientations of contacts and contact forces using two parameters  $R$  and  $\Theta$ . For simplification, orientations of contacts and contact forces are collectively denoted as contact orientations throughout the paper.

Specifically, the sphere center (point  $O$  in Fig.1) of stereographic projection is arbitrarily selected in space. According to the mapping principle of stereographic projection, each contact orientation (vectors  $OA$  and  $OD$  in Fig. 1) in a granular assembly can be projected to a point (points  $C$  and  $F$  in Fig. 1) on the equatorial plane, one contact orientation corresponds to one point on the equatorial plane, and one contact orientation interval corresponds to one area element (area  $Z$  in Fig.1) on the equatorial plane. The projection principle can be expressed as

$$\begin{cases} R = \tan \frac{\varphi}{2} & (0 \leq \varphi \leq \frac{\pi}{2}) \\ R = \cot \frac{\varphi}{2} & (\frac{\pi}{2} < \varphi \leq \pi) \\ \Theta = \theta. \end{cases} \quad (1)$$

Subsequently number of projections or average contact force for each area element is calculated, and contour lines of the collected values for each area element are plotted on the contact orientation distribution diagram (CODD).

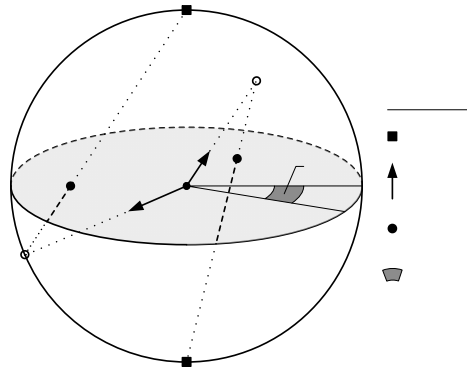


Fig. 1 – Illustration of stereographic projection of contact orientations.

By this means two kinds of CODD are defined: the one contouring number of projections for each area element is used to describe probability distribution of contact normals over all the orientation intervals and characterize contact anisotropy; the other contouring average contact force for each area element is used to describe distribution of contact forces over all the orientation intervals and characterize contact force anisotropy.

A CODD for contact anisotropy of a granular assembly is illustrated in Fig. 2b. The assembly is provided by DEM. Briefly, 40 000 spherical particles with uniform diameter of 2 units are confined in a cylindrical space whose diameter is 70 units under the gravity which is normal to projection plane, and a spherical sampling volume is defined inside the granular assembly for CODD. Probability distribution of contact normals over all the orientation intervals in the sampling volume, expressed as  $P(\mathbf{n}) = \Delta M(\mathbf{n}) / M /$

$\Delta \mathbf{n}$ , is plotted on the CODD, where  $\mathbf{n}$  denotes an orientation,  $\Delta \mathbf{n}$  denotes magnitude of the orientation interval,  $\Delta M(\mathbf{n})$  denotes the number of contacts in the orientation interval, and  $M$  denotes the total number of contacts in the sampling volume.

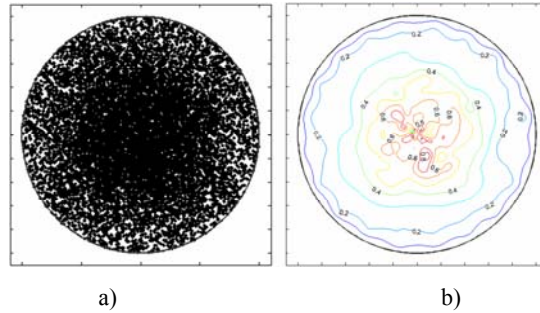


Fig. 2 – Projections and probability distributions of contact normal.

CODD illustrated in Fig. 2 involves 13481 contacts and 200 uniform orientation intervals. Number of contacts  $\Delta M(\mathbf{n})$  in each orientation interval varies within the range 2–119 with the average of about 70. As one physical contact corresponds to two contact normals in reverse directions, only the contact normals located in the domain  $z > 0$  (or  $z < 0$ ) are selected for the CODD.

## 2.2. Statistical model for contact anisotropy

In configuration of stress-force-fabric relationship (S-F-F) for granular assemblies (Ouadfel and Rothenburg, 2001), contact anisotropy is expressed as the second-order term in Fourier series of spherical harmonics of contact orientation distribution, which is an anisotropy tensor  $a_{ij}^r$

$$P(\mathbf{n}) = \frac{1}{4\pi} [1 + a_{ij}^r n_i n_j] \quad (2)$$

The definition of the anisotropy tensor is mainly for the link between macroscopic stress tensor and microscopic contact forces, and is a mechanical and macroscopic anisotropy parameter. However in this paper a group of statistical anisotropies are defined to straightforward characterize contact anisotropy in detail.

To determine the contact anisotropy in the assembly above, probability distributions of contact normals in  $\mathbf{R}$  (or  $\varphi$ ) and  $\Theta$  (or  $\theta$ ) orientations are collected and shown in Fig. 3.

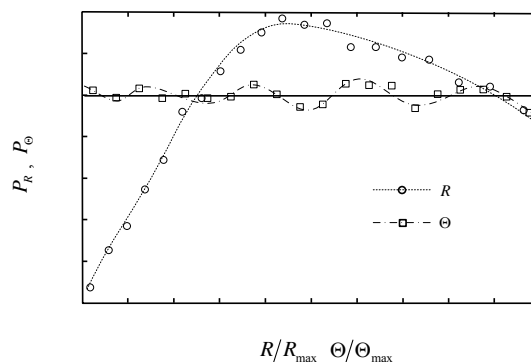


Fig. 3 – Probability distributions  $P_R$  and  $P_\Theta$  of contact normals in  $\mathbf{R}$  and  $\Theta$  orientations.

Contact anisotropies in  $\mathbf{R}$  and  $\Theta$  orientations may be expressed as

$$\begin{cases} A_R^c = \int_0^{R_{\max}} |P_R - \langle P_R \rangle| dR & , \quad \int_0^{R_{\max}} \langle P_R \rangle dR = 1 \\ A_\Theta^c = \int_0^{\Theta_{\max}} |P_\Theta - \langle P_\Theta \rangle| d\Theta & , \quad \int_0^{\Theta_{\max}} \langle P_\Theta \rangle d\Theta = 1 \end{cases} \quad (3)$$

where  $P_R$  and  $P_\Theta$  are abbreviations of  $P(\mathbf{R})$  and  $P(\Theta)$ ,  $\langle P_R \rangle$  and  $\langle P_\Theta \rangle$  denote the average of  $P_R$  and  $P_\Theta$ . Contact anisotropy for entire orientations may be represented as

$$A_n^c = \int |P(\mathbf{n}) - \langle P(\mathbf{n}) \rangle| d\mathbf{n} \quad , \quad \int \langle P(\mathbf{n}) \rangle d\mathbf{n} = 1 \tag{4}$$

where  $\langle P(\mathbf{n}) \rangle$  denotes the average of  $P(\mathbf{n})$ .

Here, a supposition is proposed that the probability distribution  $P_R$  is  $\Theta$ -independent and  $P_\Theta$  is  $R$ -independent. In this case there is no interaction between  $P_R$  and  $P_\Theta$ . Then

$$\begin{cases} P(\mathbf{n}) = \frac{P_R d\mathbf{R} \cdot P_\Theta d\Theta}{R d\mathbf{R} d\Theta} = \frac{P_R P_\Theta}{R} \\ \langle P(\mathbf{n}) \rangle = \frac{\langle P_R P_\Theta \rangle}{R} = \frac{\langle P_R \rangle \langle P_\Theta \rangle}{R} \end{cases} \tag{5}$$

In view of Eq. (5), Eq. (4) can be rewritten as

$$\tilde{A}_n^c = \iint |P_R P_\Theta - \langle P_R \rangle \langle P_\Theta \rangle| d\mathbf{R} d\Theta, \tag{6}$$

where denotes the virtual contact anisotropy under the supposition.

In accordance with the supposition, in the case that  $P_R$  is  $\Theta$ -independent and  $P_\Theta$  is  $R$ -independent. So the interaction between  $P_R$  and  $P_\Theta$  may be indicated by

$$\Delta A_n^c = \left| \tilde{A}_n^c - A_n^c \right|. \tag{7}$$

Table 1

Values of contact anisotropies in the granular assembly

Contact anisotropies	$A_R^c$	$A_\Theta^c$	$A_n^c$	$\tilde{A}_n^c$	$\Delta A_n^c$
Values	0.2622	0.0317	0.4141	0.5517	0.1376

The values of statistical contact anisotropies in the granular assembly are shown in Table 1. It is demonstrated that contact anisotropy in  $R$  orientation is extremely stronger than that in  $\Theta$  orientation, and the interaction between  $P_R$  and  $P_\Theta$  is observed.

### 2.3. Statistical model for contact force anisotropy

Different from the CODD for contact anisotropy, distribution of average normal contact forces over all the orientation intervals in the sampling volume is plotted on the CODD for contact force anisotropy. Distribution of average normal contact forces is defined as

$$E(\mathbf{n}) = \frac{\langle f^n(\mathbf{n}) \rangle}{\langle f^n \rangle} \quad , \quad \langle f^n \rangle = \int \langle f^n(\mathbf{n}) \rangle P(\mathbf{n}) d\mathbf{n}, \tag{8}$$

where  $\mathbf{n}$  denotes an orientation,  $E(\mathbf{n})$  denotes distribution of average normal contact forces,  $\langle f^n(\mathbf{n}) \rangle$  denotes average normal contact forces in the orientation interval, and  $\langle f^n \rangle$  denotes the mean value of  $\langle f^n(\mathbf{n}) \rangle$  over entire orientations.

The CODD for normal contact force anisotropy in the granular assembly is illustrated in Fig. 4a, and distributions of average normal contact forces in  $R$  (or  $\varphi$ ) and  $\Theta$  (or  $\theta$ ) orientations are collected and shown in Fig. 4b.

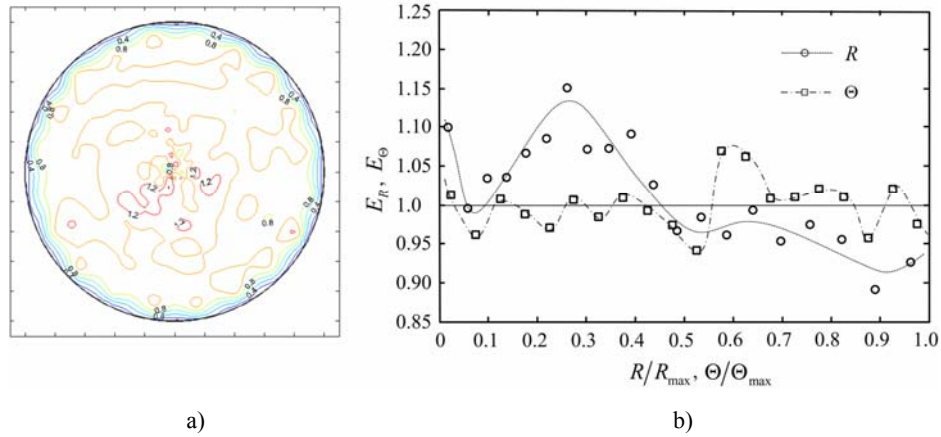


Fig. 4 – CODD for normal contact force anisotropy and distributions of average normal contact forces in  $\mathbf{R}$  and  $\Theta$  orientations.

Similarly a group of statistical normal contact force anisotropies are defined as

$$\begin{cases} A_R^{f^n} = \int_0^{R_{\max}} |E_R - \langle E_R \rangle| d\mathbf{R} & , \quad \langle E_R \rangle = \int_0^{R_{\max}} E_R P(\mathbf{R}) d\mathbf{R} = 1 \\ A_\Theta^{f^n} = \int_0^{\Theta_{\max}} |E_\Theta - \langle E_\Theta \rangle| d\Theta & , \quad \langle E_\Theta \rangle = \int_0^{\Theta_{\max}} E_\Theta P(\Theta) d\Theta = 1 \end{cases} \quad (9)$$

where  $E_R$  and  $E_\Theta$  are abbreviations of  $E(\mathbf{R})$  and  $E(\Theta)$ ,  $\langle E_R \rangle$  and  $\langle E_\Theta \rangle$  denote the average of  $E_R$  and  $E_\Theta$ .

$$A_n^{f^n} = \int |E(\mathbf{n}) - \langle E(\mathbf{n}) \rangle| d\mathbf{n}, \quad \langle E(\mathbf{n}) \rangle = \int E(\mathbf{n}) P(\mathbf{n}) d\mathbf{n} = 1, \quad (10)$$

where  $\langle E(\mathbf{n}) \rangle$  denotes the average of  $E(\mathbf{n})$ .

In the case that  $E_R$  (and  $P_R$ ) is  $\Theta$ -independent and  $E_\Theta$  (and  $P_\Theta$ ) is  $\mathbf{R}$ -independent, the following expression is held

$$\int E(\mathbf{n}) P(\mathbf{n}) d\mathbf{n} = \int_0^{R_{\max}} E_R P(\mathbf{R}) d\mathbf{R} \cdot \int_0^{\Theta_{\max}} E_\Theta P(\Theta) d\Theta = \iint E_R P(\mathbf{R}) E_\Theta P(\Theta) d\mathbf{R} d\Theta. \quad (11)$$

Then

$$\begin{cases} E(\mathbf{n}) = E_R E_\Theta \\ \langle E(\mathbf{n}) \rangle = \langle E_R E_\Theta \rangle = \langle E_R \rangle \langle E_\Theta \rangle \end{cases} \quad (12)$$

In view of Eq. (12), Eq. (10) can be rewritten as

$$\tilde{A}_n^{f^n} = \iint |E_R E_\Theta - \langle E_R \rangle \langle E_\Theta \rangle| R d\mathbf{R} d\Theta. \quad (13)$$

The interaction between  $A_R^{f^n}$  and  $A_\Theta^{f^n}$  may be indicated by

$$\Delta A_n^{f^n} = \left| \tilde{A}_n^{f^n} - A_n^{f^n} \right|. \quad (13)$$

Table 2

Values of normal contact force anisotropies in the granular assembly

Normal contact force anisotropies	$A_R^{f^n}$	$A_\Theta^{f^n}$	$A_n^{f^n}$	$\tilde{A}_n^c$	$\Delta A_n^{f^n}$
Values	0.0564	0.0247	0.1190	0.0601	0.0589

Values of statistical normal contact force anisotropies in the granular assembly are shown in Table 2. It is demonstrated that normal contact force anisotropy in  $\mathbf{R}$  orientation is approximately equal to that in  $\mathbf{\Theta}$  orientation. The interaction between and is observed but very weak.

As a summary of the calculated results on the contact anisotropy and normal contact force anisotropy in the granular assembly, it can be concluded that orientations of contacts but not contact forces dominate the anisotropy in the case of the provided boundary conditions and loading conditions.

### 3. RESULTS AND DISCUSSIONS

#### 3.1. Statistical contact anisotropies in random dense arrangements generated with different methods

Generally two kinds of methods are used to generate random dense arrangements of spherical particles: one is ‘geometrical’ method such as Jodrey-Tory algorithm (Jodrey and Tory, 1985; Anikeenko *et al.*, 2008); the other is ‘mechanical’ method such as DEM (Cundall and Strack, 1979). The ‘geometrical’ method is usually adopted in physics to observe the microstructure in a random dense pack. The ‘mechanical’ method is always used to study the micro and macro mechanics in a granular assembly. As the mechanical information can not be provided by the ‘geometrical’ method, in this section only statistical contact anisotropies are compared between the random dense arrangements given by the modified Jodrey-Tory algorithm and DEM.

For comparison, the simulations with the two methods are both performed in a cylinder whose diameter is 10 units. Two random dense arrangements of 15 000 spherical particles with uniform diameter of 0.39832927829832 units are generated in the cylinder. Gravity in DEM and translation in Jodrey-Tory algorithm are adopted for the densification of the arrangements. The diameter of particles is unknown before simulation for Jodrey-Tory algorithm, so Jodrey-Tory algorithm is performed first and DEM is performed later using the calculated diameter in the Jodrey-Tory algorithm. In the DEM  $\mathbf{R}$  and  $\mathbf{\Theta}$  orientations are both assigned wall boundary condition, and in the Jodrey-Tory algorithm  $\mathbf{R}$  orientation is assigned periodic boundary. CODD for contact anisotropies in the two random dense arrangements are illustrated in Fig. 5.

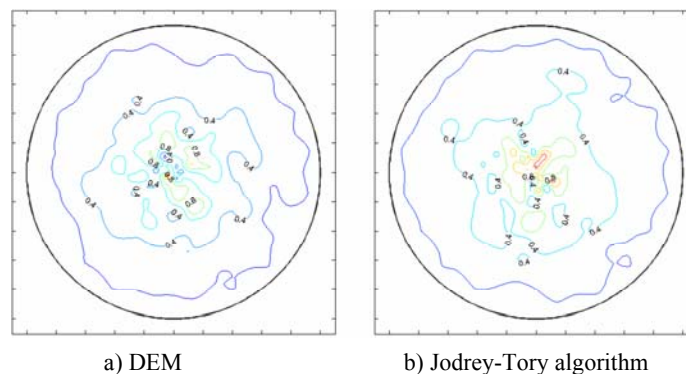


Fig. 5 – CODD for contact anisotropies in the two particle arrangements generated with DEM and modified Jodrey-Tory algorithm.

Contact anisotropies in the two random dense arrangements are clearly and precisely illustrated in CODD. It can be seen from Fig. 5 that in the two particle arrangements contact anisotropies present a similar distribution, and contact anisotropies in  $\mathbf{R}$  orientation make the major contributions.

Table 3

Contact anisotropies in the two particle arrangements with DEM and Jodrey-Tory algorithm

Contact anisotropies	$A_R^c$	$A_{\Theta}^c$	$A_n^c$	$\tilde{A}_n^c$	$\Delta A_n^c$
DEM	0.2457	0.0617	0.4480	0.5368	0.0888
Modified Jodrey-Tory algorithm	0.2674	0.0572	0.3849	0.6447	0.2598

Values of statistical contact anisotropies in the two random dense arrangements generated with DEM and modified Jodrey-Tory algorithm are collected in Table 3. From comparison it can be concluded that the entire contact anisotropy in the arrangement with modified Jodrey-Tory algorithm is smaller than that with DEM, however has larger anisotropy in  $\mathbf{R}$  orientation and significant interaction between  $\mathbf{R}$  and  $\Theta$  orientations. The difference between the results with the two methods may be attributed to inferences of ‘geometrical’ and ‘mechanical’.

### 3.2. Statistical contact anisotropies in random dense arrangements generated with different boundaries using modified Jodrey-Tory algorithm

As the densification of arrangement is controlled by mechanics in DEM, wall boundary is always used. To observe the effects of boundaries on the contact anisotropy, modified Jodrey-Tory algorithm is adopted for its flexibility of boundary.

Briefly, two particle arrangements are generated: one in a cylinder with wall boundary in  $\Theta$  orientation and periodic boundary in  $\mathbf{R}$  orientation; the other in a cube with periodic boundaries in  $\mathbf{x}$ ,  $\mathbf{y}$  and  $\mathbf{z}$  orientations. Here the particle arrangement in section 3.1 is used as the one in a cylinder with hybrid boundary. CODD for contact anisotropies in the two random dense arrangements are illustrated in Fig. 6.

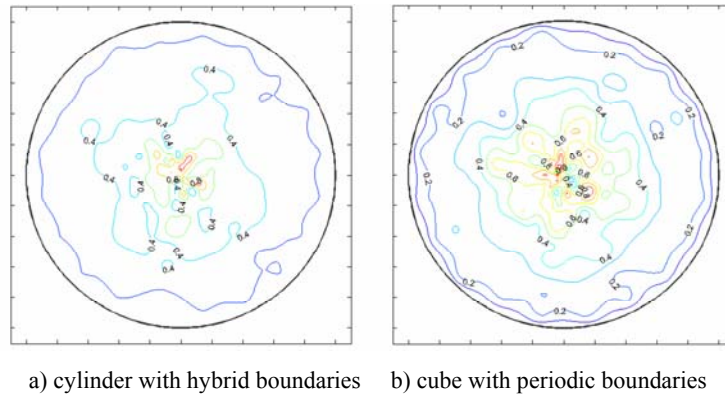


Fig. 6 – CODD for contact anisotropies in the two particle arrangements generated with different boundaries.

It can be seen from Fig. 6 that there are slight differences between the contact anisotropy distributions in the two particle arrangements. Values of statistical contact anisotropies in the two random dense arrangements are collected in Table 4.

Table 4

Contact anisotropies in the two particle arrangements with different boundaries

Contact anisotropies	$A_R^c$	$A_\Theta^c$	$A_n^c$	$\tilde{A}_n^c$	$\Delta A_n^c$
Cylinder with hybrid boundaries	0.2674	0.0572	0.3849	0.6447	0.2598
Cube with periodic boundaries	0.2638	0.0422	0.3825	0.5913	0.2088

Obviously all the indicators for contact anisotropies for the arrangement in a cube with periodic boundaries in  $x$ ,  $y$  and  $z$  orientations are more satisfactory, even compared to the indicators for DEM in Table 3. Random dense arrangement with periodic boundaries generated by Jodrey-Tory algorithm is relatively appropriate for observation of geometry for its superior isotropy.

### 3.3. Statistical contact force anisotropies in random dense arrangements generated with different densification procedures using DEM

Generally in most simulations of DEM, random dense arrangements are created with two approaches: one is to place a required number of particles (with diameters much smaller than their final size) into a

domain of interest, then the particle diameters are gradually increased until a dense arrangement is reached; the other is to assign the final size to the particles and place them into a large domain, then the particles are moved by gravity-driven or moving-wall-driven.

To observe the effects of densification procedures on the contact force anisotropy, two random arrangements with different densification procedures (gravity-driven deposition and gradually-increasing diameter) are studied. Here the particle arrangement in section 2.1 is adopted as the one using gradually-increasing diameter to perform densification procedure. CODD for normal contact force anisotropies in the two particle arrangements are illustrated in Fig. 7.

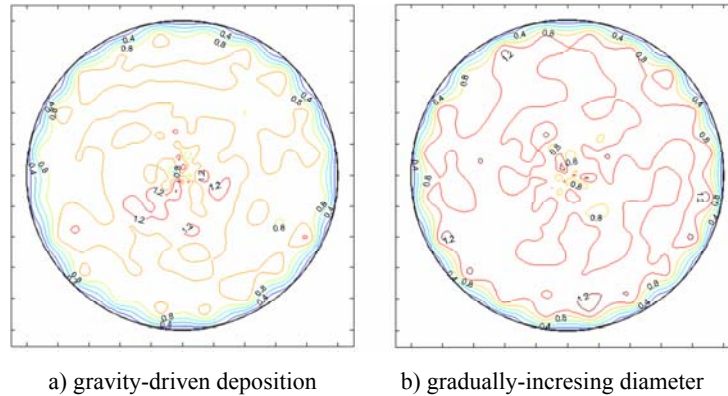


Fig. 7 – CODD for contact anisotropies in the two particle arrangements generated with different boundaries.

Values of statistical contact force anisotropies in the two particle arrangements are collected in Table 5.

Table 5

Normal contact force anisotropies in the two particle arrangements with different densification procedures

Normal contact force anisotropies	$A_R^{f^n}$	$A_\Theta^{f^n}$	$A_n^{f^n}$	$\tilde{A}_n^{f^n}$	$\Delta A_n^{f^n}$
Gravity-driven deposition	0.0564	0.0247	0.1190	0.0601	0.0589
Gradually-increasing diameter	0.0391	0.0338	0.0976	0.0422	0.0554

From comparison it can be concluded from Fig. 7 and Table 5 that the random arrangement using gradually-increasing diameter as densification procedure has a little better isotropy.

#### 4. CONCLUSIONS

In this paper contact orientation distribution diagram (CODD) for illustrating anisotropy in granular materials is proposed, and a group of statistical indicators are developed to determine anisotropy. The statistical indicators are introduced to compare anisotropies in different granular assemblies which are simulated with different existing methods, under different boundaries and using different densification procedures. The results of comparisons demonstrate that:

- (1) As a typical ‘geometrical’ method to generate random dense arrangement of spherical particles, Jodrey-Tory algorithm has a better performance in entire isotropy than DEM. But as a typical ‘mechanical’ method, DEM has a better overall performance in all the statistical indicators.
- (2) For random dense arrangements created with Jodrey-Tory algorithm, periodic boundaries in  $x$ ,  $y$  and  $z$  orientations are relatively appropriate for observation of microscopic geometry, because the particle arrangement has a better isotropy.
- (3) For random arrangements simulated with DEM, the densification procedure of gradually-increasing diameter is more beneficial for contact force isotropy of the arrangement than gravity-driven deposition.

## REFERENCES

1. Bernal, J.D., Mason, J., *Co-ordination of randomly packed spheres*, Nature, 188, pp. 910–911, 1960.
2. Agnolin, I., Roux, J.N., *Internal states of model isotropic granular packings. I. Assembling process, geometry, and contact networks*, Physical Review, E **76**, 061302, 2007.
3. Liu, C., Nagel, S.R., Schecter, D.A., Coppersmith, S.N., Majumdar, S., Narayan, O., Witten, T.A., *Force fluctuations in bead packs*, Science, **269**, pp. 513–515, 1995.
4. Kruyt, N.P., Rothenburg, L., *Probability density functions of contact forces for cohesionless frictional granular materials*, International Journal of Solids and Structures, **39**, pp. 571–583, 2002.
5. Bagi, K., *Statistical analysis of contact force components in random granular assemblies*, Granular Matter, **5**, pp. 45–54, 2003.
6. Trentadue, F., *A rigid-plastic micromechanical modeling of a random packing of frictional particles*, International Journal of Solids and Structures, **48**, pp. 2529–2535, 2011.
7. Liu, Hai, Zhang, Shi-Hong, Cheng, Ming, Song, Hong-Wu, Trentadue, F., *A minimum principle for contact forces in random packings of elastic frictionless particles*, Granular Matter, **17**, pp. 475–482, 2015.
8. Radjai, F., Jean, M., Moreau, J.J., Roux, S., *Force distributions in dense two-dimensional granular systems*, Physical Review Letters, **77**, pp. 274–277, 1996.
9. Silbert, L.E., Grest, G.S., Landry, J.W., *Statistics of the contact network in frictional and frictionless granular packings*, Physical Review, E **66**, 061303, 2002.
10. Nemat-Nasser, S., *A micromechanically-based constitutive model for frictional deformation of granular materials*, Journal of the Mechanics and Physics of Solids, **48**, pp. 1541–1563, 2000.
11. He, Q.-C., *On the micromechanical definition of macroscopic strain and strain-rate tensors for granular materials*, Computational Materials Science, **94**, pp. 51–57, 2014.
12. Horne, M.R., *The behaviour of an assembly of rotund rigid cohesionless particles I and II*, Proceedings of The Royal Society London, Series A **286**, pp. 62–97, 1965.
13. Ouadfel, H., Rothenburg, L., *‘Stress-force-fabric’ relationship for assemblies of ellipsoids*, Mechanics of Materials, **33**, pp. 201–221, 2001.
14. Majumdar, T.S., Behringer, R.P., *Contact force measurements and stress-induced anisotropy in granular materials*, Nature, **435**, pp. 1079–1082, 2005.
15. Azema, E., Radjai, F., *Internal Structure of Inertial Granular Flows*, Physical Review Letters, **112**, 078001, 2014.
16. Cundall, P.A., Drescher, A., Strack, O.D.L., *Numerical experiments on granular assemblies: measurement and observations*, in: Vermeer, P.A., Luger, H.J. (Eds.), Proceedings of the IUTAM Conference on Deformation and Failure of Granular Materials, Delft. Balkema, Rotterdam, 1982, pp. 355–370.
17. Thornton, C., Barnes, D.J., *Computer simulated deformation of compact granular assemblies*, Acta Mechanica, **64**, pp. 45–61, 1986.
18. Rothenburg, L., Bathurst, R.J., *Analytical study of induced anisotropy in idealized granular materials*, Geotechnique, **39**, pp. 601–614, 1989.
19. Cundall, P.A., Strack, O.D.L., *Modeling of microscopic mechanisms in granular materials*, in: Jenkins, J.T., Satake, M. (Eds.), Mechanics of Granular Materials: New Model and Constitutive Relations. Elsevier, Amsterdam, pp. 137–149, 1983.
20. Jodrey, W.S., Tory, E.M., *Computer simulation of close random packing of equal spheres*, Physical Review, A **32**, pp. 2347–2351, 1985.
21. Anikeenko, A.V., Medvedev, N.N., Aste, T., *Structural and entropic insights into the nature of the random-close-packing limit*, Physical Review, E **77**, 031101, 2008.
22. Cundall, P.A., Strack, O.D.L., *Discrete numerical-model for granular assemblies*, Geotechnique, **29**, pp. 47–65, 1979.

Received January 15, 2018